



Contents lists available at ScienceDirect

Journal of King Saud University – Science

journal homepage: www.sciencedirect.com

Original article

Facile fabrication of malonic acid capped silver nanoparticles and their antibacterial activity

Irshad Begum^a, Fuad Ameen^{b,*}, Zahid Soomro^a, Sana Shamim^c, Saleh AlNadhari^d, A. Almansob^b, Ahmed Al-Sabri^b, Afsheen Arif^e^a Department of Chemistry, University of Karachi, Karachi 75270, Pakistan^b Department of Botany & Microbiology, College of Science, King Saud University, Riyadh 11451, Saudi Arabia^c Dow College of Pharmacy (DCOP), Dow University of Health Sciences (DUHS), Karachi 75270, Pakistan^d Department of Plant Protection, College of Agriculture, King Saud University, Riyadh, Saudi Arabia^e The Karachi Institute of Biotechnology and Genetic Engineering, University of Karachi, Karachi 75270, Pakistan

ARTICLE INFO

Article history:

Received 16 September 2020

Revised 30 September 2020

Accepted 31 October 2020

Available online 11 November 2020

Keywords:

Silver nanoparticles
Tri sodium citrate
Sodium borohydride
Malonic acid
Capping

ABSTRACT

The successful management of infections caused by human pathogenic bacteria is becoming a challenge for clinicians. Therefore, new strategies to circumvent the growth of pathogens need to be developed. The current study was therefore aimed to synthesize silver nanoparticles (AgNPs) through chemical reduction process of silver nitrate by tri sodium citrate or sodium borohydride and evaluated their antibacterial activity. During the synthesis process, AgNPs were capped by malonic acid (a dicarboxylic acid). We have exploited two approaches of cold (reduction by NaBH₄) and hot (reduction by trisodium citrate) process for the synthesis of AgNPs which revealed maximum absorbance of AgNPs at 412 nm and 397 nm respectively. The malonic acid (MA) functionalized AgNPs (AgNPs/MA) were systematically characterized for their size, surface changes and morphology. These colloidal AgNPs were stable and polydisperse in nature with an average diameter of 20 nm. The zeta potential (ZP) analysis showed stable AgNPs. The AgNPs synthesis was optimized in a set of different reactions where concentration of metal precursor, concentration of capping agent, temperature, time of stirring and duration of reaction were variable. The AgNPs/MA were found poly-dispersed in nature with predominantly spherical shape. The antibacterial potential of AgNPs was then assessed against both Gram positive (*Staphylococcus aureus*) and Gram negative bacteria (*Escherichia coli*, *Pseudomonas aeruginosa*, *Salmonella typhi*, and *Klebsiella pneumoniae*) by antimicrobial disc susceptibility assay with three replicates per treatment which showed promising antibacterial activity of AgNPs. The AgNPs/MA possessing remarkably smaller size exhibited encouraging antibacterial activity against human bacterial pathogens suggesting their potential application in controlling bacterial infections in clinical settings and can be utilized in further biomedical applications.

© 2020 The Authors. Published by Elsevier B.V. on behalf of King Saud University. This is an open access article under the CC BY-NC-ND license (<http://creativecommons.org/licenses/by-nc-nd/4.0/>).

1. Introduction

The miniature world of nanotechnology and nanoparticles possesses tremendous applications in various fields, and it is one of the dynamic and fastest growing interdisciplinary area (Isacfranklin et al., 2020; Swathi et al., 2020). Metallic nanoparti-

cles have been utilized for many industrial and domestic applications including medical diagnosis, biosensor, agriculture, therapeutics, personal care products and pharmaceuticals (Ali et al., 2019; Haroon et al., 2019). Nanoparticles possess some intriguing features remarkably distinct from their bulk materials (Rajput et al., 2020). These include smaller size, higher surface area, catalytic efficiency, higher surface energy, absorption in visible region, etc. (Ahmed et al., 2017) which increase their therapeutic potential to cure certain diseases or treat disease causing organisms with no or both biologically and statistically insignificant side effects (Sanna and Sechi, 2020). Therefore, the fabrication of novel, smaller sized nanoparticles with defined shape is envisaged in developing effective antibacterial agents to successfully control or curb the pathogenic invasions (Valarmathi et al.,

* Corresponding author.

E-mail address: fuadameen@ksu.edu.sa (F. Ameen).

Peer review under responsibility of King Saud University.



<https://doi.org/10.1016/j.jksus.2020.101231>

1018-3647/© 2020 The Authors. Published by Elsevier B.V. on behalf of King Saud University.

This is an open access article under the CC BY-NC-ND license (<http://creativecommons.org/licenses/by-nc-nd/4.0/>).

2020). Also, the morphological engineering of nanoparticles modifies their photocatalytic, chemo-biological and optical properties (Khan et al., 2019). Considering these cutting edge properties and utilization of metal nanoparticles in various fields, several methods such as chemical, electrochemical, chemical vapor deposition, reduction by ionizing radiation, molecular beam epitaxial, and chemical reduction methods with and without stabilizing polymers have been explored for nanoparticles synthesis (Abou El-Nour et al., 2010; Rane et al., 2018). Among these, chemical reduction method using a reducing and a capping agent has been followed by many researchers (Ahari et al., 2018; Shenava, 2013). This capping approach offer certain following economic benefits- (i) cost effective methods and (ii) the chemical method can be easily scaled up.

Among the metallic nanoparticle, AgNPs exhibit unique properties of optical, surface plasmon behavior, electronic and magnetic behavior (Irvani et al., 2014). It has modifiable mechanical and chemical properties. They also account for more than 55% commercial value in total nanomaterial based products (Agnihotri et al., 2014). AgNPs' size may range from 8 to 100 nm. In the last two decades, AgNPs have gained valuable attention due to their unique physiochemical properties including but not limited to good conductivity, chemical stability, and catalytic activity. The AgNPs have also widely been used as antibacterial and antifungal agents with low or nil cytotoxicity to animal cells (Shu et al., 2020).

Every year, infections caused by pathogenic bacterial species affect a large population of humans globally which raises serious concerns over deadly bacterial infections and their available treatments (Ahmed et al., 2019). On the other hand, development of drug resistance in pathogenic bacteria to many available antibiotics has further aggravated the problem (Hamilton et al., 2020). Therefore, the quest for novel and effective antibacterial nanoparticles becomes a need of the hour, help reducing the pathogenic invasions and their adverse clinical outcomes in a cost effective manner. In this regard, metal nanoparticles have shown significant growth inhibitory or killing effects against drug resistant microbial pathogens originally isolated from diseased human samples and therefore, have been suggested as new generation material combating pathogenic infections (Ameen et al., 2020a, 2020b). From the array of metal nanoparticles, AgNPs in particular, are of great importance and have proven to be useful as new nanoantibiotics (Ameen et al., 2019) due to their unique but superior features (Helmlinger et al., 2016). Besides, the antibacterial impact of AgNPs is better than other metallic nanoparticles while exerting very little negative influence on mammalian cells (Ivask et al., 2014). Due to the abovementioned set of unique features and biocidal activity, the AgNPs can effectively assist as antibiotic alternative or supplement to antibiotic therapy against multidrug resistant bacteria including the strains of Gram negative *Escherichia coli*, *Pseudomonas aeruginosa* and Gram positive *Staphylococcus aureus* (Ahmed et al., 2019; Ali et al., 2018). Silver can destruct the bacterial cells both in nanoparticle form or Ag^+ ions released from AgNPs. Mechanistically, AgNPs cause bacterial cell death as the following sequence of events: (i) binding of Ag^+ to negatively charged surface of cell membrane altering cell membrane potential and morphology (Ahmed et al., 2018), (ii) interruption of respiratory chain, (iii) induction of intracellular oxidative stress, (iv) leakage of cytoplasmic content (Tripathi et al., 2017), and (iv) inhibition of virulence factors like exopolysaccharides, quorum sensing and biofilm formation (Shah et al., 2019). Antibacterial nature of AgNPs with oligodynamic action, broad spectrum microbial killing and lower chances of development of resistance against them make the AgNPs a robust candidate for antibacterial applications (Shenava, 2013). The synthesis is more dependent on controlled size, shape and stability in dispersion system. For AgNPs synthesis, sodium borohydride (NaBH_4) is a well-known strong reducing

agent, utilized to achieve small and uniform sized silver colloids. In contrast, trisodium citrate is a weaker reducing agent resulting in large sized AgNPs. Malonic acid ($\text{CH}_2(\text{COOH})_2$) is a dicarboxylic acid and malonates are the esters and salts of malonic acid and its ionized form. The name originates from the Greek word $\mu\alpha\lambda\omicron\nu$ (*malon*) meaning 'apple'. Malonic acid has pendant ionized groups that are capable to reduce the metal ions and form stable nanoparticles. The stability and size of nanoparticles plays a decisive role in determining their antibacterial potential (Tamiyakul et al., 2019). Recently, some researchers have prepared and stabilized AgNPs by using some carboxylic acids. For instance, a polymeric dispersant and a short chain carboxylic acid was used to prepare AgNPs (Titkov et al., 2018). Similarly, citric acid and gallic acid mediated AgNPs were synthesized recently (Kalaivani et al., 2016; Lunkov et al., 2020). Organic acids possess a carboxylic ($-\text{COOH}$) group which undergoes transformation in solution and releases a proton (H^+) and an electron (e^-) (Shankar and Rhim, 2015). The electrons released from $-\text{COOH}$ groups reduce the silver metal ions (Ag^+) to zero valent form (Ag^0). Moreover, if a reducing agent like NaBH_4 or trisodium citrate is used, they also strongly reduce the Ag^+ ions. After reduction, $-\text{COO}^-$ can stabilize the surface of positively charged silver atoms.

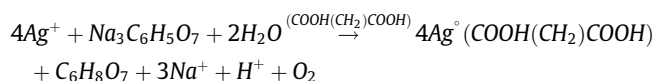
Considering the importance of malonic acid and facile AgNPs, the current work was designed to systematically accomplish the following goals- (i) synthesis of malonic acid capped AgNPs (AgNPs/MA) (ii) characterization of AgNPs by SEM, FT-IR and UV-visible spectroscopy and (iii) assessment of antibacterial potential of AgNPs/MA against five major bacterial pathogens including *E. coli*, *K. pneumoniae*, *P. aeruginosa*, *S. typhi*, and *S. aureus*.

2. Materials and methods

Two main synthesis methods namely cold (reduction by NaBH_4) and hot (reduction by trisodium citrate) process were implemented in this research work to produce AgNPs. The sodium borohydride and trisodium citrate were used as reducing agents for the reduction of silver ions (Ag^+) to AgNPs. Reaction parameters like temperature, molar concentration, stirring time, and pH were optimized during the fabrication of AgNPs. The relative quantities and concentrations of metal precursor, concentration of capping agents, temperature, time for stirring and duration of reactions were performed.

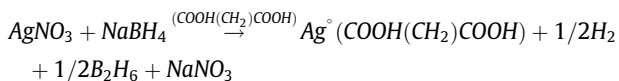
2.1. Synthesis of capped AgNPs/MA

Silver precursor i.e. silver salt (AgNO_3) was prepared by Turkevich method which provides free Ag^+ ions in reaction medium. Trisodium Citrate ($\text{Na}_3\text{C}_6\text{H}_5\text{O}_7$) was incorporated as the reducing agent and malonic acid was applied as capping agent. In a 10 mL capacity flask, 1 mL of 4 mM Tri Sodium Citrate was added first and heated to 70 °C, then dropwise mixture of 0.1 M NaOH (0.5 mL) and malonic acid (7 mL) was added under vigorous stirring on magnetic stirrer, for 10 min. A total of 1 mL silver nitrate solution (10%) was added dropwise in the mixture. The content was stirred for another 15 min or till the color changes to pale yellow. The color change was observed from colorless to bright yellow.



In another set of synthesis experiment, NaBH_4 was used as reducing agent followed by capping with malonic acid to produce AgNPs/MA. Ice-chilled 2 mM NaBH_4 (1 mL) was added to a 10 mL reaction flask and a mixture of solutions (7 mL of malonic acid

solution and 0.5 mL of 0.1 M NaOH) was added dropwise under constant stirring. Later, 1 mL (10%, of AgNO₃ solution) was added dropwise.



The solution turned from colorless to bright yellow and was attributed to formation of AgNPs. The synthesized AgNPs/MA solution was stored in the dark at 4 °C. The resultant product was analyzed by UV–Vis spectrophotometer (Model number UV-1800 Parma Spec., Shimadzu, Japan), in the absorbance range of 300–800 nm wavelength (Yan et al., 2014).

2.2. Characterization of AgNPs

AgNPs/MA formation was monitored by UV–Vis spectroscopy with an increase in surface plasmon resonance (SPR) till the end of reaction, whereas, dry powder of AgNPs/MA was characterized by Fourier transform infrared (FT-IR) spectroscopy, scanning electron microscopy (SEM), transmission electron microscopy (TEM), dynamic light scattering (DLS) and zeta-potential analyses.

2.3. Ultraviolet–Visible absorption spectroscopy (UV–Vis)

The photosensitive properties were acquired using UV–Vis spectrophotometer (Model # UV-1800 Parma Spec., Shimadzu, Japan). After adding the reducing and capping agent in a predefined set of volumes, the color change from transparent to light brown was observed and spectra were recorded. Various reaction mixtures were prepared varying the molar concentration of AgNO₃, malonic acid, time of reaction, and pH of reaction mixture.

2.4. Fourier transform infrared spectroscopy (FT-IR)

After standardizing the reaction parameters, best combination of molarity, pH, and time for the synthesis of trisodium citrate and NaBH₄ mediated and MA capped AgNPs was selected and the ultimate product was dried in a vacuum oven at 60 °C to obtain the fine powder of AgNPs. The obtained powder was characterized by employing FT-IR technique to reveal the adsorption of functional groups on the surface of AgNPs. The FT-IR analysis was performed on Shimadzu IR-Prestige-21 for functional groups. The spectral working range was 400–4000 cm⁻¹. The sample discs for FT-IR were prepared following KBr disc preparation method on Model # EX-54175JMU.

2.5. Scanning and transmission electron microscopy (SEM/TEM) of AgNPs

SEM analysis was carried out to determine the surface morphology of AgNPs/MA and size distribution of particle aggregates through SEM Model:JSM 6380A, JEOL Ltd, Japan. The fine powder of AgNPs was stick on to a double sided carbon tape on aluminum stubs and visualized under SEM at an accelerating voltage of 15 kV for morphological analysis and to measure the diameter of particle aggregates. For observing shape and diameter of AgNPs, TEM analysis was performed. Copper grids were prepared using a small volume of water dispersed AgNPs. After drying the Cu-grid for at least 6 h at 80 °C, the microscopy was performed and size of AgNPs was calculated based on the observation of diameter.

2.6. Dynamic light scattering and zeta-potential analysis of AgNPs

To check the aggregation behavior of synthesized AgNPs in solution, the hydrodynamic size was determined. Hydrodynamic

size plays a key role in biological activities of nanoparticles in solution. Also, it provides the information about toxicological profile of a nanoparticle (Khurana et al., 2014). The DLS and zeta potential measurements were carried out in double distilled water at a concentration of 50 µg/ml of AgNPs to assess the hydrodynamic size and net positive or negative potential.

2.7. Antimicrobial susceptibility test

Disc diffusion method described earlier (Ameen et al., 2020) was used to evaluate the antimicrobial efficacy of AgNPs/MA. The potency of AgNPs/MA was checked alone and in synergism with other some antibiotics such as azithromycin, sparfloxacin, ciprofloxacin, gemifloxacin, and ofloxacin was performed by using disk susceptibility technique (Kirby et al., 1966). The discs were loaded with AgNPs/MA by disc soaking method using micropipette. A 50 µl of AgNPs/MA solution from stock concentration of 1 mg/ml was used to be absorbed by discs. Discs loaded with AgNPs/MA were placed in the petri dishes containing sterile Muller-Hinton agar with bacterial cultures uniformly spread over it. A 0.5 McFarland standard (1.0 × 10⁸ CFU/ml) bacterial cultures were used for the assay. Antibiotics, nanoparticles and silver nitrates paper discs were prepared by soaking them in 100 ppm solution of drugs, followed by drying. Petri dishes were then incubated at 36 °C ± 1 °C, for 24 h. Each experiment was performed in triplicates. Zones of inhibition were carefully measured using digimatic calipers in millimeters (Mitutoyo Rochester, NewYork) (K and J, 2017).

3. Results

3.1. Ultraviolet–Visible absorption spectroscopy (UV–Vis)

3.1.1. Synthesis of AgNPs/MA generated by hot process (reduction by trisodium citrate)

Synthesis of AgNPs was performed with various combinations of AgNO₃ (0.5–1 mM) and MA molarities (0.25–4 mM), time (1–10 min.) and pH (3–11). Three AgNO₃ concentrations (0.5 mM, 0.75 mM and 1.0 mM) were added to MA concentrations 0.25, 2.12 and 4.0 mM and observed for 5, 10 and 15 min. The maximum absorbance of AgNPs was recorded as 412 nm. The optimized conditions were found as: 0.5 mM AgNO₃ with 2.12 mM MA for 5 min (Fig. 1a); 0.75 mM AgNO₃ with 2.12 mM MA for 10 min. (Fig. 1b); and 1 mM AgNO₃ with 2.12 mM for 15 min. (Fig. 1c). Whereas pH 11 shows the optimum synthesis of capped AgNPs (Fig. 1d).

3.2. Synthesis of AgNPs/MA generated by cold process (reduction by NaBH₄)

Similarly, three AgNO₃ concentrations (0.5 mM, 0.75 mM and 1.0 mM) were mixed with three concentrations of MA (0.25 mM, 2.12 mM and 4.0 mM) in various combinations and observed for 1 to 3 min. The AgNPs maximally absorbed the incidence light at 397 nm. The data revealed optimum production of AgNPs in the following amalgamations: (i) 0.5 mM AgNO₃ + 4 mM MA with a reaction time of 1 min. (Fig. 2a), (ii) 0.75 mM + 2.12 mM MA for 3 min. (Fig. 2b), and (iii) 1 mM AgNO₃ + 4 mM with a reaction time of 35 min. (Fig. 2c). While assessing the impact of reaction pH, pH 11 maximally enhanced the production of AgNPs followed by pH 8 and pH 9 (Fig. 2d).

3.3. Fourier transform infrared spectroscopy (FT-IR)

FT-IR measurements were performed to recognize the major functional groups adsorbed on to the surface of AgNPs. The FT-IR data revealed the role of tri sodium citrate and MA functional

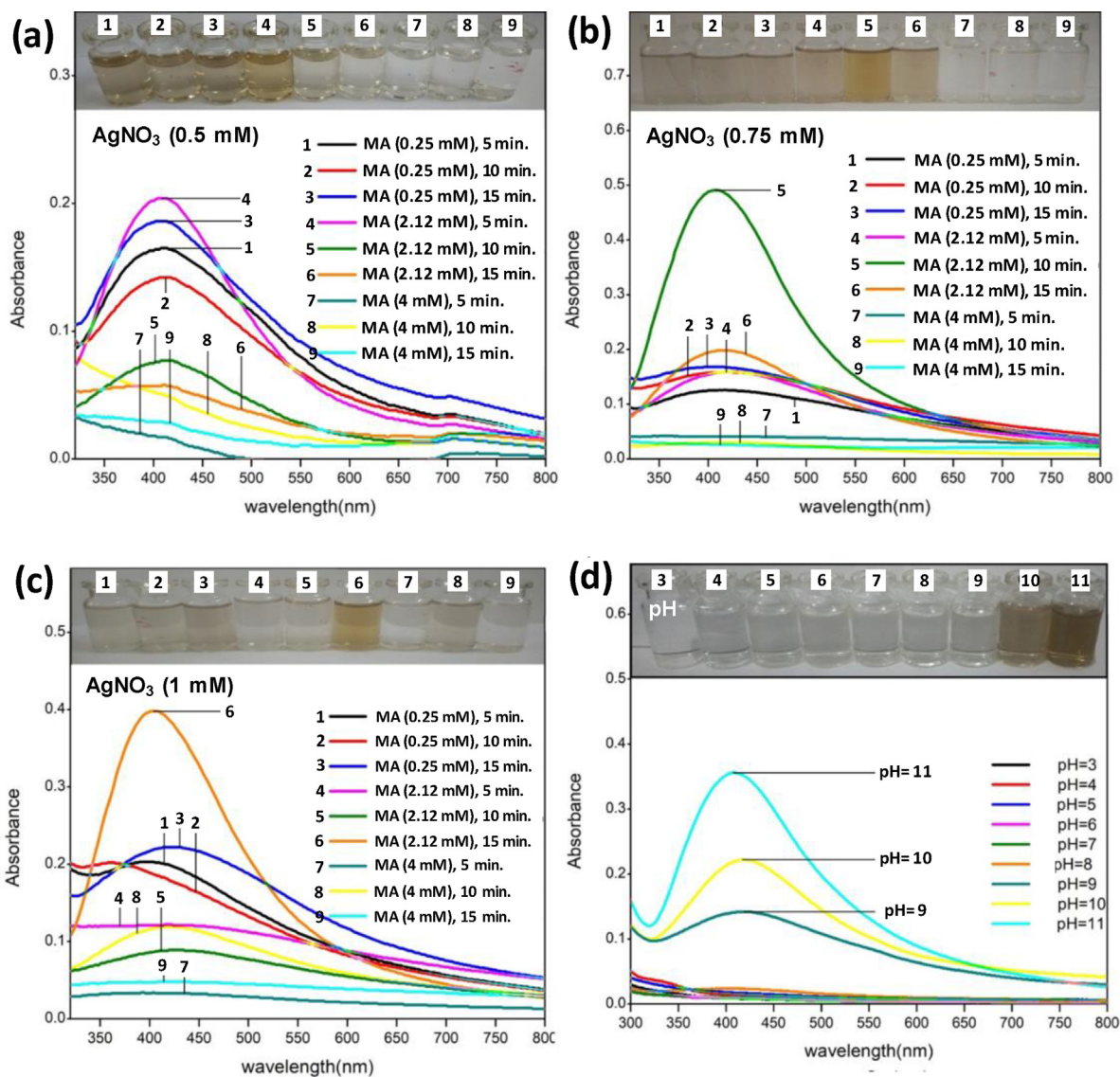


Fig. 1. UV-vis spectroscopic analyses of AgNPs as a function of different combinations of AgNO₃ and malonic acid molarity and time (Panels a–c) and pH of reaction medium (panel D). The evidence of color change is presented at the top of each panel denoted with same letters as can be seen in the respective spectrum. The increasing hyperchromic shift shows increasing surface plasmon resonance (SPR) of AgNPs/MA reduced by trisodium citrate under variable reaction condition.

groups in effective capping of AgNPs. The FT-IR vibration assignment of MA, TSC, and their AgNPs are presented in Table 1. The peaks at 3462 cm⁻¹ and 3485 cm⁻¹ were very strong and broad and could be assign to the hydroxyl groups (-OH). CO stretching vibration was found in MA at 1311 and 1172 cm⁻¹ which were also present in C-AgNPs/MA. As per a scattering study of neutrons (Bougeard et al., 1988) the broad signal at 3105 cm⁻¹ was due to two dimer rings of malonic acid (related to two identical >C=O groups of malonic acid). A prominent and sharp peak observed at 1637 cm⁻¹ (Fig. 3) and 1639 cm⁻¹ (Fig. 4) appeared due to stretching of carbonyl (>C=O) group.

3.4. Dynamic light scattering and zeta potential

DLS analysis determined the colloidal nature of AgNPs in the suspension with only one signal between 10 and 100 nm (Fig. 5a, b). Z-average size distribution curve provided the information that synthesized and stabilized H-AgNPs/MA and C-AgNPs/MA were poly-dispersed in nature, with average diameter of 123.6 nm and 111.4 nm, respectively and PDI value were measured as 0.488

and 0.468 for H-AgNPs/MA and C-AgNPs/MA, respectively (Fig. 5a,b).

3.5. Zeta potential

The analysis was conducted on Nano ZS zetasizer system (Malvern Instruments) and the surface potential was found to be -21.3 mV and -13.5 mV for H-AgNPs/MA and C-AgNPs/MA, respectively (Fig. 5c,d).

3.6. Scanning and transmission electron microscopy

The synthesized and capped AgNPs were predominantly spherical in shape. The average size based on the 50 readings of individual nanoparticles showed an average size of 20 nm by TEM (Fig. 6a). The diameter of the nanoparticle aggregates was found less than 100 nm in size by SEM. The SEM images also suggested that the produced nanoparticles were uniform in shape (Fig. 6b).

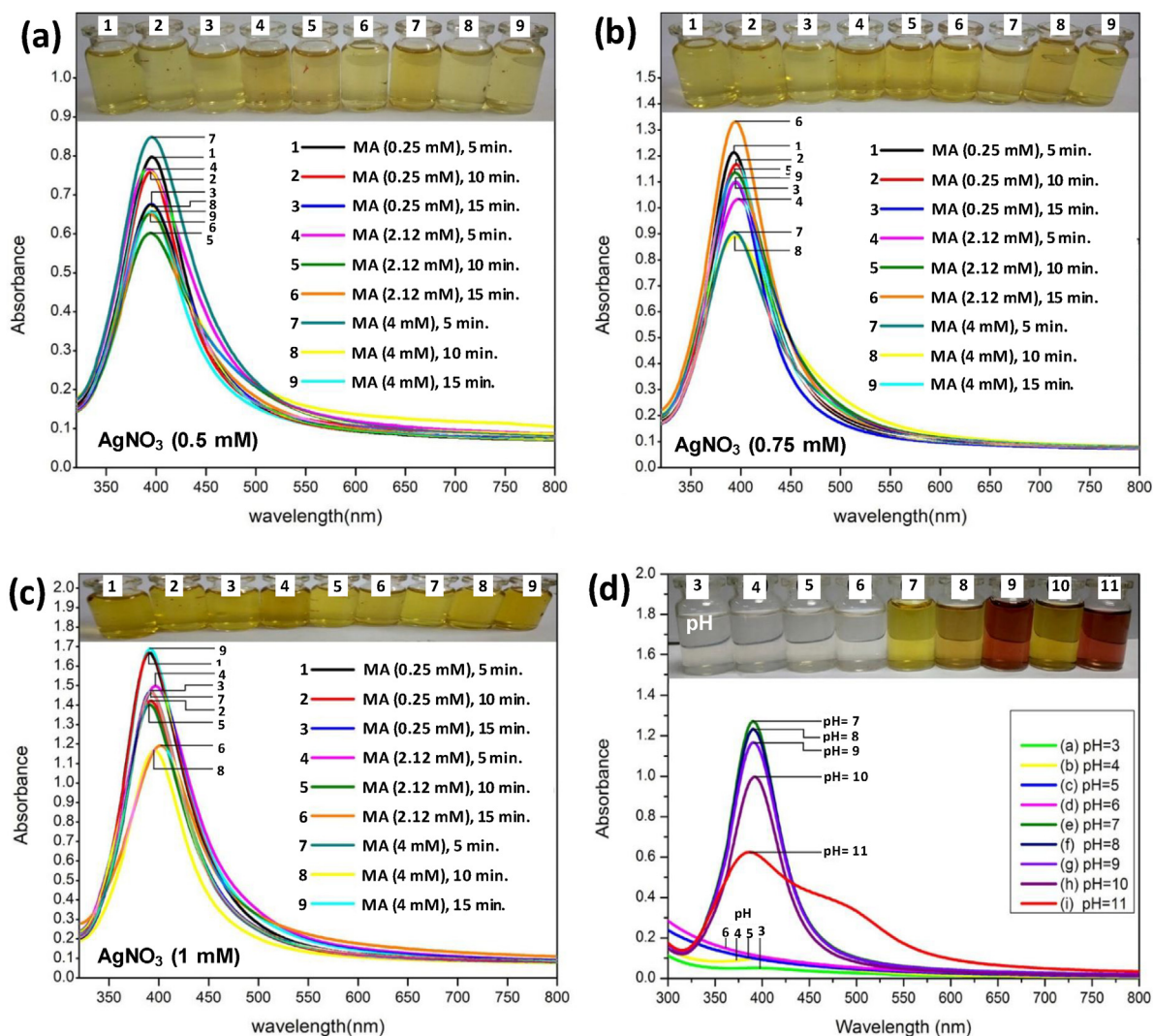


Fig. 2. UV-vis spectroscopic analyses of AgNPs as a function of different combinations of AgNO₃ and malonic acid molarity and time (panels a–c) and pH of reaction medium (panel D). The evidence of color change is presented at the top of each panel denoted with same letters as can be seen in the respective spectrum. The increasing hyperchromic shift shows increasing surface plasmon resonance (SPR) of AgNPs/MA reduced by sodium borohydride under variable reaction condition.

3.7. Antimicrobial susceptibility test

Azithromycin with C-AgNPs/MA showed high antibacterial activity against *Pseudomonas aeruginosa* with NaBH₄ and C-AgNPs/MA with TSC remained the same. *Escherichia coli* increased from 1 to 1.5 for NaBH₄, as well as it was more susceptibility to TSC. In *Salmonella* it decreased. Antimicrobial activity was increased for *Klebsiella pneumoniae*, for both the AgNPs with sodium borohydride and above 2.5 for TSC (Fig. 7a). For the antibiotic sparfloxacin, the C-AgNPs/MA showed high antibacterial activity against gram negative bacteria which experienced more reduction than with TSC, these nanoparticles worked well against *P. aeruginosa*, *E.coli* and *K. pneumoniae*, and it showed a zone of inhibition of as 3 mm. (Fig. 7b). In case of ciprofloxacin, the AgNPs does not any remarkable change for resistant, the results are almost same for both AgNO₃ and NaBH₄, AgNPs (Fig. 8a). For the antibiotic gemifloxacin, the C-AgNPs/MA and TSC showed antibacterial activity well against *Pseudomonas aeruginosa* and not any other organism (Fig. 8b). The C-AgNPs did not show significant antibacterial activity against ofloxacin (Fig. 9).

4. Discussion

The successful eradication of drug resistant clinical bacteria associated with acute and chronic infections is gradually becoming a serious issue and pose challenges to management of infectious diseases due to the flexible or resilient nature of causal microorganism (Yelin and Kishony, 2018). As per the reports, approximately 70% human bacterial pathogens have become resistant to single or combination of antibacterial drugs (Ansari et al., 2014) and biofilm forming bacteria among them cause 80% infectious diseases (Kalia et al., 2019). To overcome the multi drug resistance problem, the new class of antibacterial agents are urgently required. In this context, AgNPs have the potential to profoundly reduce the drug resistance and increased bacterial killing by AgNPs alone or in synergy with antibiotics. To this end, five pathogenic bacterial strains were grown in the presence of newly fabricated AgNPs/MA and AgNPs/citrate established and the results showed growth inhibiting potential of AgNPs. The toxicity pattern towards bacterial cells was variable which could be due the structural composition of bacterial cells and cell wall thickness. Similar to our

Table 1
FT-IR peak assignment of MA, TSC, C-AgNPs/MA, and C-AgNPs/TSC.

Vibration	Major IR signal in malonic acid (MA)	Major IR signals in C-AgNPs/MA	Reference	Vibration	Major IR signal in tri sodium citrate (TSC)	Major IR signals in C-AgNPs/TSC	Reference
O-H stretching	3105	3485	(Thorat et al., 2018)	O-H stretching	3034	3462	(Thottoli and Unni, 2013)
Carbonyl stretching	1696	1637	(Thorat et al., 2018)	Carbonyl stretching	1718	1639	(Thorat et al., 2018)
deformation CH	1411	1462	(Movasaghi et al., 2008)	C-H bending	1435	1537	(Thottoli and Unni, 2013)
C-O stretching	1311	1386	(Thottoli and Unni, 2013)	C-O stretching	1311	-	(Thottoli and Unni, 2013)
CO stretching	1172	1124	(Movasaghi et al., 2008)	C-H bending	910	-	(Thottoli and Unni, 2013)
C-H bending	912	1043	(Thottoli and Unni, 2013)	C-H bending	765	-	(Thottoli and Unni, 2013)
C-H bending	771		(Thottoli and Unni, 2013)	C-H deformation	651	634	(Thottoli and Unni, 2013)
C-H deformation	655		(Thottoli and Unni, 2013)				

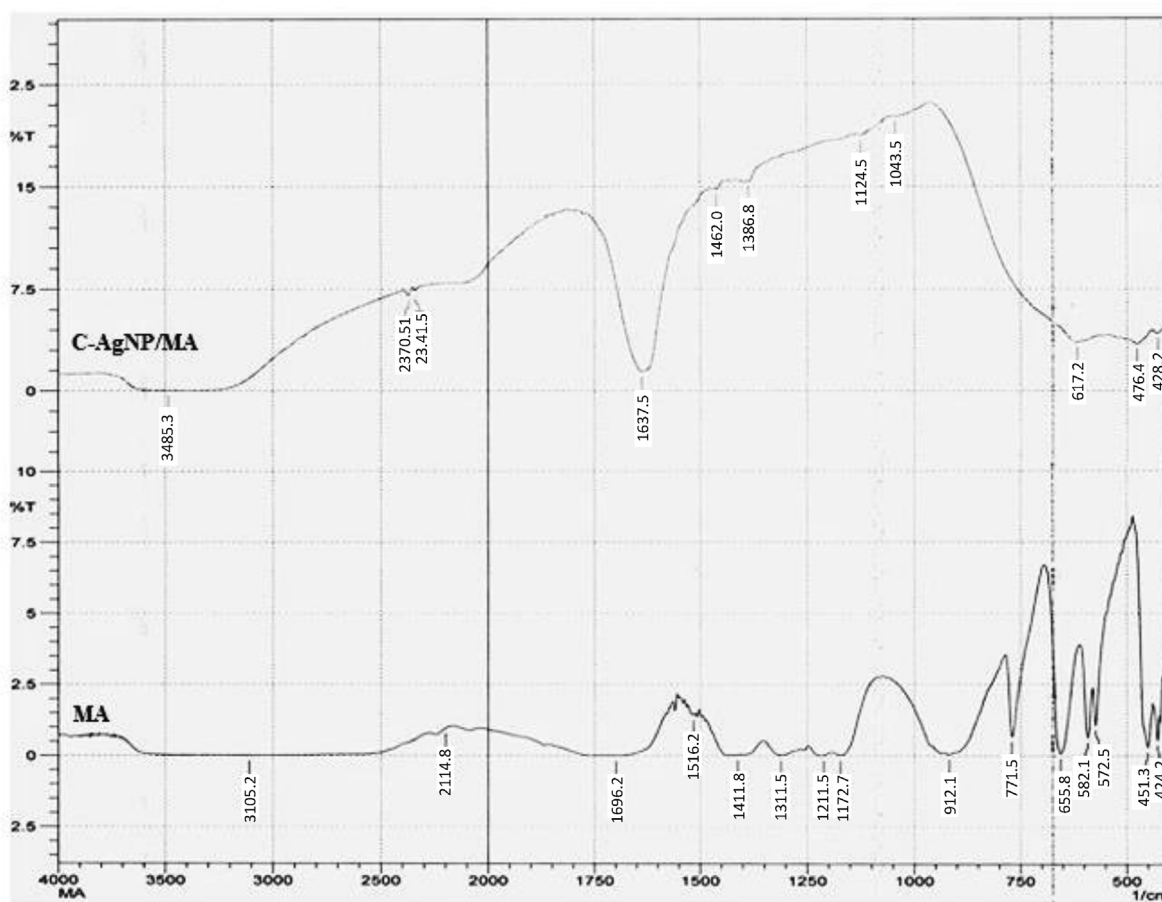


Fig. 3. FT-IR spectral representation of capped AgNPs reduced by trisodium citrate.

study, the bactericidal impact of AgNPs have also been reported recently on *E. coli*, *S. aureus*, *K. pneumoniae*, *S. typhi*, *B. cereus*, *P. aeruginosa*, and *P. mirabilis* (Huang et al., 2020; Kambale et al., 2020; Mohanta et al., 2020). AgNPs also releases Ag⁺ ions in the medium which simultaneously with AgNPs induce a double sword impact on bacterial cells (Durán et al., 2016). The silver ions due to electrostatic interactions with negatively charged teichoic acids adversely affect bacterial cells. Due to thick peptidoglycan (PG) layer, Gram positive bacteria such as *S. aureus* are less susceptible than Gram negative bacteria. On the other hand, bacteria belonging to Gram negative genera experience more destruction due to less

PG content. The negatively charged lipopolysachchrides (LPS) of Gram negative bacteria also promote adsorption of AgNPs and which increases the bacterial killing by multi folds (Dakal et al., 2016). Although, antibacterial mechanisms have been explored in great detail and the available literature on AgNP's killing effect suggests that AgNPs are able to inhibit the electron transport in cellular membranes altering membrane permeability and creating new pores which induces more intracellular uptake of AgNPs and oxidative stress (Ahmed et al., 2018). Simultaneously, sulphur and phosphorus containing molecules become one of the targets of AgNPs, for instance, nucleic acids and proteins

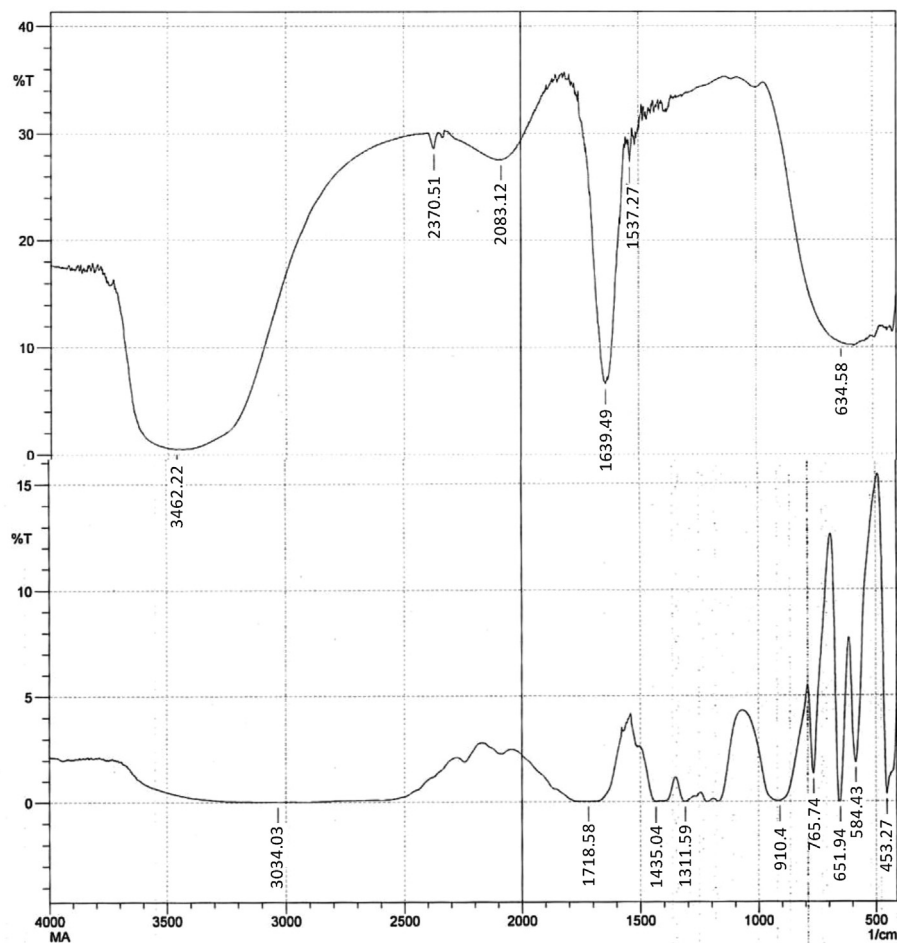


Fig. 4. FT-IR spectral representation of capped AgNPs reduced by sodium borohydride.

are inactivated by the action of AgNPs (Chernousova and Epple, 2013). Also, the generation of free radicals and uncoupling of oxidative phosphorylation lead to bacterial cell killing (Saleem et al., 2017).

Due to these antibacterial actions, AgNO₃ has found numerous biomedical applications (Tarannum et al., 2019). Fabrication of AgNPs was done by using reducing agents like sodium borohydride and tri sodium citrate and followed by capping with malonic acid. The polydispersed, colloidal and capped AgNPs showed significant antibacterial activity with NaBH₄ against *P. aeruginosa* due to their expanded surface area. To the best of our knowledge these are first AgNPs capped with malonic acid and well characterized by UV-Vis, FTIR, DLS, SEM/TEM and zeta potential. The colloidal AgNPs/MA were also effective against both gram positive and gram-negative bacteria. These results can be corroborated with earlier studies (Mythili et al., 2018; Saravanan et al., 2018). The DLS analysis showed the colloidal nature of AgNPs in the suspension with only one signal between 10 and 100 nm which are close to those obtained for AgNPs prepared by sodium citrate method (Jeong et al., 2014). Dispersion or distribution of AgNPs in colloidal solution can be revealed by polydispersity index analysis. The polydispersity index value between 0.1 and 0.3 denotes stable AgNPs dispersion with low frequency of particle aggregation (Ardani et al., 2017; De Melo et al., 2020). In our study, the PDI value were measured as 0.488 and 0.468 for H-AgNPs/MA and C-AgNPs/MA, respectively which suggest high polydisperse nature of AgNPs (Ardani et al., 2017). The mechanism of AgNPs/MA fabrication

and its antibacterial activity can be summarized in the following steps. Carboxylic groups of malonic acid release electrons in the medium which reduces Ag⁺ ions liberating from AgNO₃ and produces zero-valent silver (Ag⁰). The color change of the reaction medium could be due to the increasing surface plasmon resonance (SPR) which consistently increases depending upon the concentration of Ag⁺ ions, malonic acid, tri sodium citrate, temperature, time, and pH until the reaction stops. The zero-valent silver atoms forms aggregates being controlled by malonic acid capping and restricted to a defined size and termed malonic acid capped AgNPs, which however would have formed large size and unstable AgNPs in the absence of malonic acid. The interactions during the capping may involve Van der Waals force of attraction, electrostatic interaction, and co-valent bond formation. When cells of five bacterial pathogens *E. coli*, *P. aeruginosa*, *K. pneumoniae*, *S. typhi*, and *S. aureus* were exposed to AgNPs, the antibacterial action of AgNPs could be due to the following steps of cell penetration and toxicity by AgNPs- adsorption, intracellular uptake, destruction of cell membrane thereby generating reactive oxygen species (ROS), leakage of cellular materials like nucleic acids, proteins, enzymes, etc., eventually leading to death of bacterial cells. Broadly, positively charged Ag⁺ ions released from AgNPs are attracted by negatively charged sulphur (S) and phosphorus (P) containing cell envelope or intracellular molecules such as membrane lipids, proteins, and nucleic acids which leads to bacterial cell deformation followed by loss of metabolism and cell death (Akter and Huq, 2020; Garibo et al., 2020).

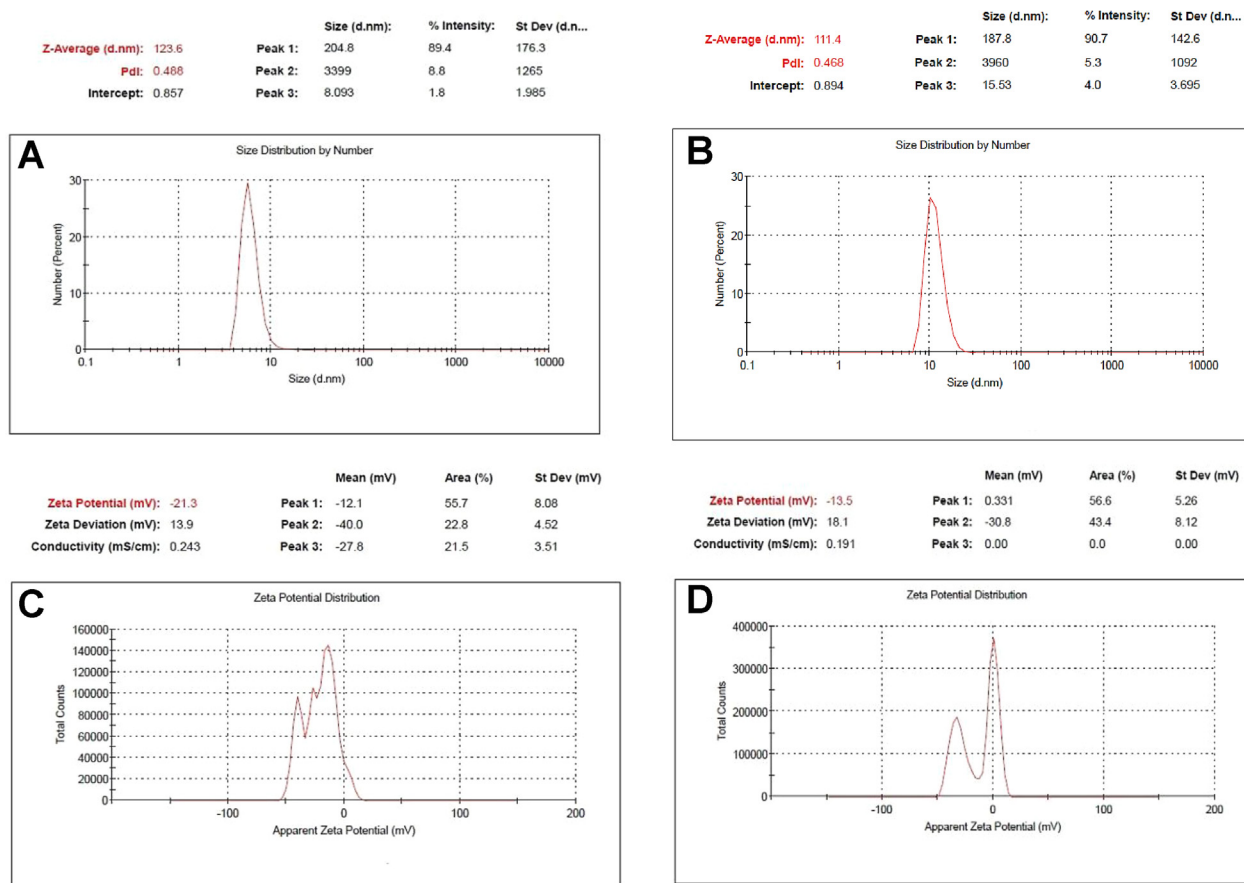


Fig. 5. Size distribution by number (percent) measured by DLS analysis of capped AgNPs reduced with A) tri sodium citrate and B) sodium borohydride, and zeta potential (ZP) analysis of capped AgNPs reduced with C) tri sodium citrate and D) sodium borohydride.

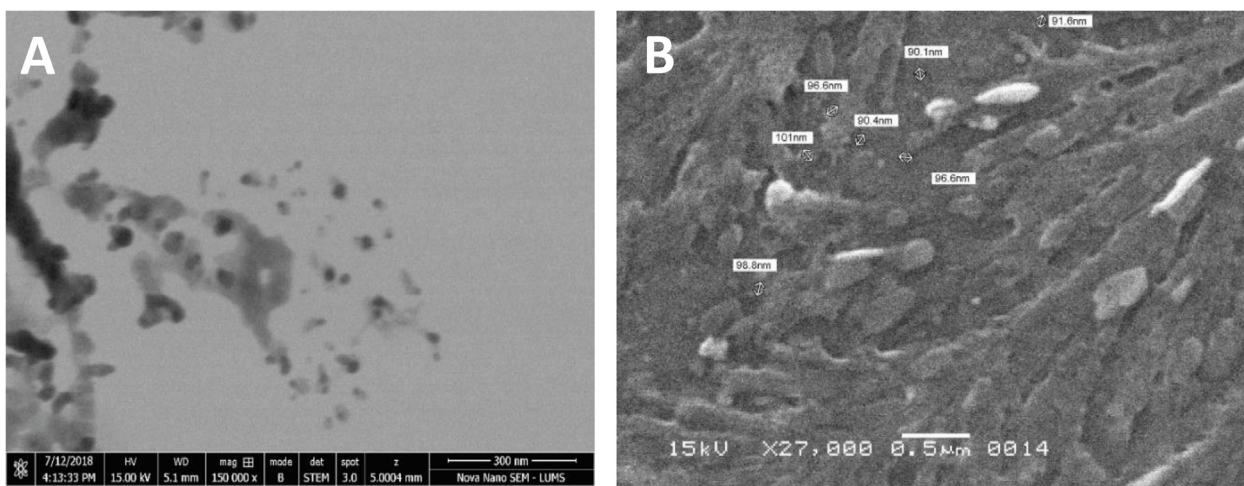


Fig. 6. Scanning electron micrographs of capped AgNPs reduced with a) tri sodium citrate and b) sodium borohydride.

5. Conclusion

In the present study, the synthesis of AgNPs with the help of malonic acid capping was observed. AgNPs showed antibacterial effects against several Gram positive and Gram negative bacteria. Due to the synergistic effect of the AgNPs with the antibiotics like ofloxacin, sparfloxacin, ciprofloxacin, gemifloxacin, and azithromy-

cin the antibacterial performance of antibiotics was enhanced. Azithromycin with C-AgNPs/MA showed maximum antibacterial activity against *P. aeruginosa* with NaBH₄. AgNPs were stable and polydisperse in nature with substantially low diameter at nanoscale. Negative zeta potential suggested that AgNPs were not agglomerated which was one of the reason of good antibacterial activity of AgNPs. Conclusively, the malonic acid capped AgNPs

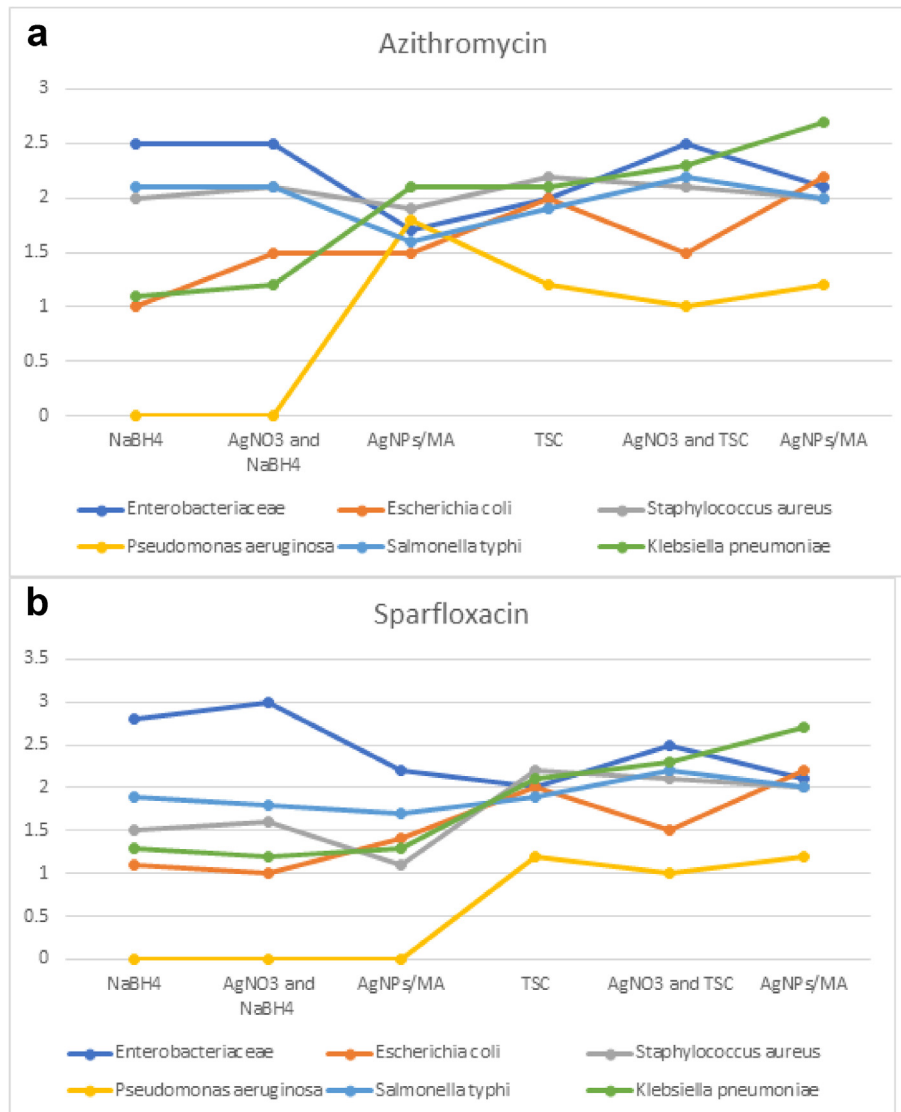


Fig. 7. Antibiotics susceptibility test for azithromycin (a) and sparfloxacin (b).

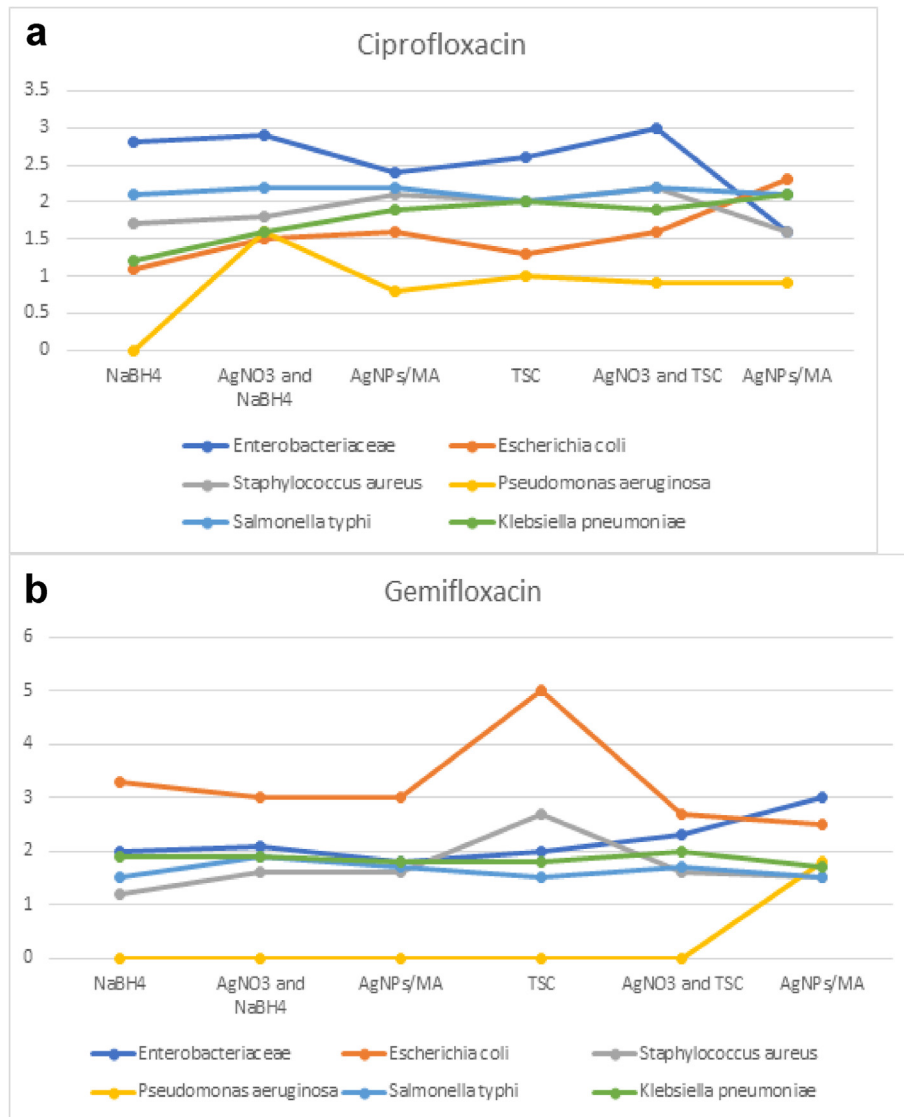


Fig. 8. Antibiotics susceptibility test for ciprofloxacin (a) and gemifloxacin.

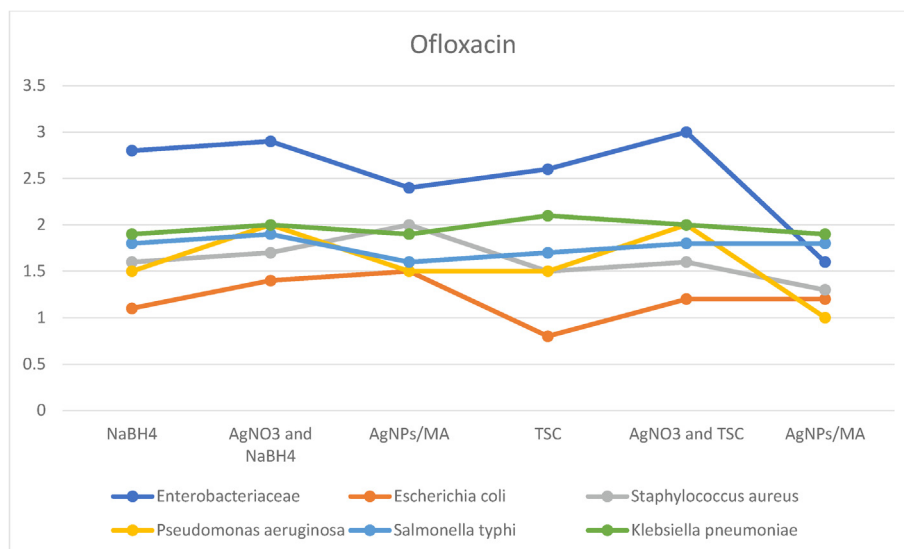


Fig. 9. Antibiotics susceptibility test for Ofloxacin.

produced through an inexpensive and fast reaction could be a suitable alternative of ineffective antibiotics and can be applied in different applications.

Declaration of Competing Interest

The authors declare that they have no known competing financial interests or personal relationships that could have appeared to influence the work reported in this paper.

Acknowledgment

The authors extend their appreciation to the Deputyship for Research & Innovation, “Ministry of Education” in Saudi Arabia for funding this research work through the project number IFKSURG-1438-029.

References

- Abou El-Nour, K.M.M., Eftaiha, A., Al-Warthan, A., Ammar, R.A.A., 2010. Synthesis and applications of silver nanoparticles. *J. Chem. Arab.* <https://doi.org/10.1016/j.arabjc.2010.04.008>.
- Agnihotri, S., Mukherji, S., Mukherji, S., 2014. Size-controlled silver nanoparticles synthesized over the range 5–100 nm using the same protocol and their antibacterial efficacy. *RSC Adv.* 4, 3974–3983. <https://doi.org/10.1039/c3ra44507k>.
- Ahari, H., Karim, G., Anvar, A.A., Pooyamanesh, M., Sajadi, A., Mostaghim, A., Heydari, S., 2018. Synthesis of the silver nanoparticle by Chemical reduction method and preparation of nanocomposite based on AgNPs, in: Proceedings of the World Congress on Mechanical, Chemical, and Material Engineering. <https://doi.org/10.11159/icpc.125>
- Ahmed, B., Dwivedi, S., Abdin, M.Z., Azam, A., Al-Shaeri, M., Khan, M.S., Saquib, Q., Al-Khedhairi, A.A., Musarrat, J., 2017. Mitochondrial and Chromosomal Damage Induced by Oxidative Stress in Zn²⁺ Ions, ZnO-Bulk and ZnO-NPs treated Allium cepa roots. *Sci. Rep.* 7, 40685. <https://doi.org/10.1038/srep40685>.
- Ahmed, B., Hashmi, A., Khan, M.S., Musarrat, J., 2018. ROS mediated destruction of cell membrane, growth and biofilms of human bacterial pathogens by stable metallic AgNPs functionalized from bell pepper extract and quercetin. *Adv. Powder Technol.* 29, 1601–1616. <https://doi.org/10.1016/j.apt.2018.03.025>.
- Ahmed, B., Solanki, B., Zaidi, A., Khan, M.S., Musarrat, J., 2019. Bacterial toxicity of biomimetic green zinc oxide nanoantibiotic: insights into ZnONP uptake and nanocolloid-bacteria interface. *Toxicol. Res. (Camb)* 8, 246–261. <https://doi.org/10.1039/C8TX00267C>.
- Akter, S., Huq, M.A., 2020. Biologically rapid synthesis of silver nanoparticles by *Sphingobium* sp. MAH-11T and their antibacterial activity and mechanisms investigation against drug-resistant pathogenic microbes. *Artif. Cells, Nanomedicine Biotechnol.* <https://doi.org/10.1080/21691401.2020.1730390>.
- Ali, K., Ahmed, B., Ansari, S.M., Saquib, Q., Al-Khedhairi, A.A., Dwivedi, S., Alshaeri, M., Khan, M.S., Musarrat, J., 2019. Comparative in situ ROS mediated killing of bacteria with bulk analogue, Eucalyptus leaf extract (ELE)-capped and bare surface copper oxide nanoparticles. *Mater. Sci. Eng. C* 100, 747–758. <https://doi.org/10.1016/j.msec.2019.03.012>.
- Ali, K., Ahmed, B., Khan, M.S., Musarrat, J., 2018. Differential surface contact killing of pristine and low EPS *Pseudomonas aeruginosa* with Aloe vera capped hematite (α -Fe₂O₃) nanoparticles. *J. Photochem. Photobiol. B Biol.* 188, 146–158. <https://doi.org/10.1016/j.jphotobiol.2018.09.017>.
- Ameen, F., Abdullah, M.M.S., Al-Homaidan, A.A., Al-Lohedan, H.A., Al-Ghanayem, A. A., Almansob, A., 2020. Fabrication of silver nanoparticles employing the cyanobacterium *Spirulina platensis* and its bactericidal effect against opportunistic nosocomial pathogens of the respiratory tract. *J. Mol. Struct.* 1217, <https://doi.org/10.1016/j.molstruc.2020.128392> 128392.
- Ameen, F., AlYahya, S., Govarthanan, M., Aljahlid, N., Al-Enazi, N., Alshamary, K., Alshehri, W.A., Alwakeel, S.S., Alharbi, S.A., 2020. Soil bacteria *Cupriavidus sp.* mediates the extracellular synthesis of antibacterial silver nanoparticles. *J. Mol. Struct.* 1202, 127233.
- Ameen, F., Srinivasan, P., Selvakumar, T., Kamala-Kannan, S., Al Nahari, S., Almansob, A., Dawoud, T., Govarthanan, M., 2019. Phytosynthesis of silver nanoparticles using *Mangifera indica* flower extract as bioreductant and their broad-spectrum antibacterial activity. *Bioorg. Chem.* 88, <https://doi.org/10.1016/j.bioorg.2019.102970> 102970.
- Ansari, M.A., Khan, H.M., Khan, A.A., Ahmad, M.K., Mahdi, A.A., Pal, R., Cameotra, S.S., 2014. Interaction of silver nanoparticles with *Escherichia coli* and their cell envelope biomolecules. *J. Basic Microbiol.* 54, 905–915. <https://doi.org/10.1002/jobm.201300457>.
- Ardani, H.K., Imawan, C., Handayani, W., Djuhana, D., Harmoko, A., Fauzia, V., 2017. Enhancement of the stability of silver nanoparticles synthesized using aqueous extract of *Diospyros discolor* Willd. leaves using polyvinyl alcohol, in: IOP Conference Series: Materials Science and Engineering. <https://doi.org/10.1088/1757-899X/188/1/012056>.
- Bougeard, D., de Villepin, J., Novak, A., 1988. Vibrational spectra and dynamics of crystalline malonic acid at room temperature. *Acta Part A Mol. Spectrosc. Spectrochim.* [https://doi.org/10.1016/0584-8539\(88\)80170-3](https://doi.org/10.1016/0584-8539(88)80170-3).
- Chernousova, S., Epple, M., 2013. Silver as antibacterial agent: Ion, nanoparticle, and metal. *Angew. Chem – Int. Ed.* <https://doi.org/10.1002/anie.201205923>.
- Dakal, T.C., Kumar, A., Majumdar, R.S., Yadav, V., 2016. Mechanistic basis of antimicrobial actions of silver nanoparticles. *Front. Microbiol.* 7, 1831. <https://doi.org/10.3389/fmicb.2016.01831>.
- De Melo, A.P.Z., De Oliveira Brisola Maciel, M.V., Sganzerla, W.G., Da Rosa Almeida, A., De Armas, R.D., MacHado, M.H., Da Rosa, C.G., Nunes, M.R., Bertoldi, F.C., Barreto, P.L.M., 2020. Antibacterial activity, morphology, and physicochemical stability of biosynthesized silver nanoparticles using thyme (*Thymus vulgaris*) essential oil 2020 Res. Express Mater. <https://doi.org/10.1088/2053-1591/ab6c63>.
- Durán, N., Durán, M., de Jesus, M.B., Seabra, A.B., Fávoro, W.J., Nakazato, G., Silver nanoparticles: A new view on mechanistic aspects on antimicrobial activity 2016 Med Nanomedicine Nanotechnology, *Biol* 10.1016/j.nano.2015.11.016
- Garibo, D., Borbón-Núñez, H.A., de León, J.N.D., García Mendoza, E., Estrada, I., Toledano-Magaña, Y., Tiznado, H., Ovalle-Marroquín, M., Soto-Ramos, A.G., Blanco, A., Rodríguez, J.A., Romo, O.A., Chávez-Almazán, L.A., Susarrey-Arce, A., 2020. Green synthesis of silver nanoparticles using *Lysiloma acapulcensis* exhibit high-antimicrobial activity. *Rep. Sci.* <https://doi.org/10.1038/s41598-020-69606-7>.
- Hamilton, K.A., Garner, E., Joshi, S., Ahmed, W., Ashbolt, N., Medema, G., Pruden, A., 2020. Antimicrobial-resistant microorganisms and their genetic determinants in stormwater: A systematic review. *Opin. Environ. Sci. Heal Curr.* <https://doi.org/10.1016/j.coesh.2020.02.012>.
- Haron, M., Zaidi, A., Ahmed, B., Rizvi, A., Khan, M.S., Musarrat, J., 2019. Effective inhibition of phytopathogenic microbes by eco-friendly leaf extract mediated silver nanoparticles (AgNPs). *Microbiol Indian J.* <https://doi.org/10.1007/s12088-019-00801-5>.
- Helmlinger, J., Sengstock, C., Groß-Heitfeld, C., Mayer, C., Schildhauer, T.A., Köller, M., Epple, M., 2016. Silver nanoparticles with different size and shape: Equal cytotoxicity, but different antibacterial effects. *RSC Adv.* 6, 18490–18501. <https://doi.org/10.1039/c5ra27836h>.
- Huang, H., Shan, K., Liu, J., Tao, X., Periyasamy, S., Durairaj, S., Jiang, Z., Jacob, J.A., 2020. Synthesis, optimization and characterization of silver nanoparticles using the catkin extract of *Piper longum* for bactericidal effect against food-borne pathogens via conventional and mathematical approaches. *Chem. Bioorg.* <https://doi.org/10.1016/j.bioorg.2020.104230>.
- Iravani, S., Korbekandi, H., Mirmohammadi, S.V., Zolfaghari, B., 2014. Synthesis of silver nanoparticles: Chemical, physical and biological methods. *Res. Pharm. Sci.*
- Isacfranklin, M., Ameen, F., Ravi, G., Yuvaakumar, R., Hong, S.I., Velauthapillai, D., Thambidurai, M., Dang, C., 2020. Single-phase Cr₂O₃ nanoparticles for biomedical applications. *Ceram. Int.* 46, 19890–19895. <https://doi.org/10.1016/j.ceramint.2020.05.050>.
- Ivask, A., Kurvet, I., Kasemets, K., Blinova, I., Arooja, V., Suppi, S., Vija, H., Kakinen, A., Titma, T., Heinlaan, M., Visnapuu, M., Koller, D., Kisand, V., Kahru, A., 2014. Size-dependent toxicity of silver nanoparticles to bacteria, yeast, algae, crustaceans and mammalian cells *in vitro*. *PLoS One* 9. <https://doi.org/10.1371/journal.pone.0102108>.
- Jeong, Y., Lim, D., Choi, J., 2014. Assessment of size-dependent antimicrobial and cytotoxic properties of silver nanoparticles. *Mater. Sci. Eng Adv.* <https://doi.org/10.1155/2014/763807>.
- K.A., J.V., 2017. Green Synthesis and Characterization of Silver Nanoparticles Using Vitex negundo (Karu Nochchi) Leaf Extract and its Antibacterial Activity. *Med. Chem. (Los Angeles)*. 07, 218–225. <https://doi.org/10.4172/2161-0444.1000460>.
- Kalaivani, G., Sivanesan, A., Kannan, A., Sevvil, R., 2016. Generating monomeric 5-coordinated microperoxidase-11 using carboxylic acid functionalized silver nanoparticles: A surface-enhanced resonance Raman scattering analysis. *Colloids Surfaces B Biointerfaces* 146, 722–730. <https://doi.org/10.1016/j.colsurfb.2016.07.017>.
- Kalia, V.C., Patel, S.K.S., Kang, Y.C., Lee, J.K., 2019. Quorum sensing inhibitors as antipathogens: biotechnological applications. *Biotechnol. Adv.* <https://doi.org/10.1016/j.biotechadv.2018.11.006>.
- Kambale, E.K., Nkanga, C.I., Mutonkole, B.P.I., Bapolisi, A.M., Tassa, D.O., Liesse, J.M.I., Krause, R.W.M., Memvanga, P.B., 2020. Green synthesis of antimicrobial silver nanoparticles using aqueous leaf extracts from three Congolese plant species (*Brilliantaisia patula*, *Crossopteryx febrifuga* and *Senna siamea*). *Heliyon* 6, e04493.
- Khan, Ibrahim, Saeed, K., Khan, Idrees, 2019. Nanoparticles: Properties, applications and toxicities. *Arab. J. Chem.* 12, 908–931. <https://doi.org/10.1016/j.arabjc.2017.05.011>.
- Khurana, C., Vala, A.K., Anandharya, N., Pandey, O.P., Chudasama, B., 2014. Antibacterial activity of silver: The role of hydrodynamic particle size at nanoscale. *J. Biomed. Mater. Res. – Part A.* <https://doi.org/10.1002/jbm.a.35005>.
- Kirby, W., Bauer, A., Sherris, J., Turk, M., 1966. Antibiotic susceptibility testing by standard single disk method. *Am. J. Clin. Pathol.* <https://doi.org/10.1080/00029157.2000.10734361>.
- Lunkov, A., Shagdarova, B., Konovalova, M., Zhukova, Y., Drozd, N., Il'ina, A., Varlamov, V., 2020. Synthesis of silver nanoparticles using gallic acid-conjugated chitosan derivatives. *Carbohydr. Polym.* 234, <https://doi.org/10.1016/j.carbpol.2020.115916> 115916.
- Mohanta, Y.K., Biswas, K., Jena, S.K., Hashem, A., Abd-Allah, E.F., Mohanta, T.K., 2020. Anti-biofilm and Antibacterial Activities of Silver Nanoparticles Synthesized by the Reducing Activity of Phytoconstituents Present in the Indian Medicinal Plant. *Microbiol Front.* <https://doi.org/10.3389/fmicb.2020.01143>.

- Mythili, R., Selvankumar, T., Kamala-Kannan, S., Sudhakar, C., Ameen, F., Al-Sabri, A., Selvam, K., Govarthan, M., Kim, H., 2018. Utilization of market vegetable waste for silver nanoparticle synthesis and its antibacterial activity. *Mater. Lett.* 225, 101–104. <https://doi.org/10.1016/j.matlet.2018.04.111>.
- Rajput, V., Minkina, T., Ahmed, B., Sushkova, S., Singh, R., Soldatov, M., Laratte, B., Fedorenko, A., Mandzhieva, S., Blicharska, E., Musarrat, J., Saquib, Q., Flieger, J., Gorovtsov, A., 2020. Interaction of copper-based nanoparticles to soil, terrestrial, and aquatic systems: Critical review of the state of the science and future perspectives. *Rev. Environ. Contam. Toxicol.* https://doi.org/10.1007/398_2019_34.
- Rane, A.V., Kanny, K., Abitha, V.K., Thomas, S., 2018. Methods for synthesis of nanoparticles and fabrication of nanocomposites. *Synthesis Inorg. Nanomater.*, 121–139 <https://doi.org/10.1016/b978-0-08-101975-7.00005-1>.
- Saleem, S., Ahmed, B., Khan, M.S., Al-Shaeri, M., Musarrat, J., 2017. Inhibition of growth and biofilm formation of clinical bacterial isolates by NiO nanoparticles synthesized from Eucalyptus globulus plants. *Microb. Pathog.* 111, 375–387. <https://doi.org/10.1016/j.micpath.2017.09.019>.
- Sanna, V., Sechi, M., 2020. Therapeutic potential of targeted nanoparticles and perspective on nanotherapies. *Chem. Lett. ACS Med.* <https://doi.org/10.1021/acsmchemlett.0c00075>.
- Saravanan, M., Gopinath, V., Chaurasia, M.K., Syed, A., Ameen, F., Purushothaman, N., 2018. Green synthesis of anisotropic zinc oxide nanoparticles with antibacterial and cytofriendly properties. *Microb. Pathog.* 115, 57–63. <https://doi.org/10.1016/j.micpath.2017.12.039>.
- Shah, S., Gaikwad, S., Nagar, S., Kulshrestha, S., Vaidya, V., Nawani, N., Pawar, S., 2019. Biofilm inhibition and anti-quorum sensing activity of phytosynthesized silver nanoparticles against the nosocomial pathogen *Pseudomonas aeruginosa*. *Biofouling*. <https://doi.org/10.1080/08927014.2018.1563686>.
- Shankar, S., Rhim, J.W., 2015. Amino acid mediated synthesis of silver nanoparticles and preparation of antimicrobial agar/silver nanoparticles composite films. *Polym. Carbohydr.* <https://doi.org/10.1016/j.carbpol.2015.05.018>.
- Shenava, A., 2013. Synthesis of silver nanoparticles by chemical reduction method and their antifungal activity. *Int. Res. J. Pharm.* 4, 111–113. <https://doi.org/10.7897/2230-8407.041024>.
- Shu, M., He, F., Li, Z., Zhu, X., Ma, Y., Zhou, Z., Yang, Z., Gao, F., Zeng, M., 2020. Biosynthesis and Antibacterial Activity of Silver Nanoparticles Using Yeast Extract as Reducing and Capping Agents. *Lett. Nanoscale Res.* <https://doi.org/10.1186/s11671-019-3244-z>.
- Swathi, S., Ameen, F., Ravi, G., Yuvakkumar, R., Hong, S.I., Velauthapillai, D., AlKahtani, M.D.F., Thambidurai, M., Dang, C., 2020. Cancer targeting potential of bioinspired chain like magnetite (Fe₃O₄) nanostructures. *Curr. Appl. Phys.* 20, 982–987. <https://doi.org/10.1016/j.cap.2020.06.013>.
- Tamiyakul, H., Roytrakul, S., Jaresitthikunchai, J., Phaonakrop, N., Tanasupawat, S., Warisnoichareon, W., 2019. Changes in protein patterns of *Staphylococcus aureus* and *Escherichia coli* by silver nanoparticles capped with poly (4-styrenesulfonic acid-co-maleic acid) polymer. *Asian Biomed.* 13, 39–47. <https://doi.org/10.1515/abm-2019-0039>.
- Tarannum, N., Gautam Divya, Y.K., 2019. Facile green synthesis and applications of silver nanoparticles: A state-of-the-art review. *RSC Adv.* 9, 34926–34948. <https://doi.org/10.1039/c9ra04164h>.
- Titkov, A.I., Shundrina, I.K., Gadirov, R.M., Odod, A.V., Kurtsevich, A.E., Yukhin, Y.M., Lyakhov, N.Z., 2018. Thermal and laser sintering of a highly stable inkjet ink consisting of silver nanoparticles stabilized by a combination of a short chain carboxylic acid and a polymeric dispersant. *Mater. Today: Proc.* 16042–16050 <https://doi.org/10.1016/j.matpr.2018.05.049>.
- Tripathi, D.K., Tripathi, A., ShwetaSingh, S., Singh, Y., Vishwakarma, K., Yadav, G., Sharma, S., Singh, V.K., Mishra, R.K., Upadhyay, R.G., Dubey, N.K., Lee, Y., Chauhan, D.K., 2017. Uptake, accumulation and toxicity of silver nanoparticle in autotrophic plants, and heterotrophic microbes: A concentric review 2017. *Microbiol Front.* <https://doi.org/10.3389/fmicb.2017.00007>.
- Valarmathi, N., Ameen, F., Almansob, A., Kumar, P., Arunprakash, S., Govarthan, M., 2020. Utilization of marine seaweed *Spyridia filamentosa* for silver nanoparticles synthesis and its clinical applications. *Mater. Lett.* 263. <https://doi.org/10.1016/j.matlet.2019.127244> 127244.
- Yan, Y., Chen, K. Bin, Li, H.R., Hong, W., Hu, X. Bin, Xu, Z., 2014. Capping effect of reducing agents and surfactants in synthesizing silver nanoplates. *Trans. Nonferrous Met. Soc. China (English Ed.)* 24, 3732–3738. [https://doi.org/10.1016/S1003-6326\(14\)63522-6](https://doi.org/10.1016/S1003-6326(14)63522-6).
- Yelin, I., Kishony, R., 2018. Antibiotic Resistance. *Cell.* <https://doi.org/10.1016/j.cell.2018.02.018>.